

FABRICATION OF DIELECTRIC $\text{Ba}_2\text{Ti}_9\text{O}_{20}$ CERAMIC BY A POLYMERIZED COMPLEX METHOD

AYHAN MERGEN

*Marmara University, Metallurgical and Materials Eng. Dept.,
Göztepe Kampüsü, 34722, Kadıköy, İstanbul, Turkey*

E-mail: ayhan.mergen@marmara.edu.tr

Submitted March 13, 2009; accepted August 24, 2009

Keywords: Microwave dielectrics ceramics, $\text{Ba}_2\text{Ti}_9\text{O}_{20}$, Polymerized complex method

Fabrication of single phase $\text{Ba}_2\text{Ti}_9\text{O}_{20}$ ceramic using the solid state reaction method is rather difficult due to thermodynamically various stable compounds that form in the vicinity of $\text{Ba}_2\text{Ti}_9\text{O}_{20}$ composition. In this study, microwave dielectric $\text{Ba}_2\text{Ti}_9\text{O}_{20}$ ceramic was successfully prepared by a polymerized complex method where crystallization of $\text{Ba}_2\text{Ti}_9\text{O}_{20}$ occurred from an amorphous polymeric mixture. Calcined powders had a particle size ranging from 10 to 50 nm with spherical shape. Single phase $\text{Ba}_2\text{Ti}_9\text{O}_{20}$ ceramic was obtained at 1200°C. The dielectric constant of $\text{Ba}_2\text{Ti}_9\text{O}_{20}$ ceramics at room temperature was around 34.5 at frequencies above 250 kHz but it significantly decreased when temperature was above 25°C.

INTRODUCTION

The development of wireless communication system brings a remarkable progress in microwave devices such as resonators and filters which are required to have small size, high-level temperature stability, and low power loss. Therefore, it is demanded that microwave dielectric materials should have a high dielectric constant ($\epsilon_r > 30$), high unload quality factor ($Q \times f > 40\,000$ GHz) and a temperature coefficient of the resonant frequency (τ_f) tunable through zero. The dielectric constant and the temperature coefficient of dielectrics in the microwave region are most likely dependent upon the compositions and crystal structures; thus it is rather difficult to control them by a slight modification of the processing route. The value of Q , however, is largely influenced by various processing factors such as purity, grain size, porosity, etc., and can therefore be increased to a high value by improving the manufacturing processes.

Several ceramic materials have been developed as microwave resonators. One of these microwave ceramics is $\text{Ba}_2\text{Ti}_9\text{O}_{20}$ which received much attention due to its good microwave properties. $\text{Ba}_2\text{Ti}_9\text{O}_{20}$ ceramic was first reported by Jonker and Kwestroo in 1958 [1] and discovered by O'Bryan and Thomson in 1970s as microwave dielectric material [2, 3]. $\text{Ba}_2\text{Ti}_9\text{O}_{20}$ microwave ceramic has a high dielectric constant ($\epsilon_r = 39.8$), good quality factor ($Q \times f = 8\,000$ at 4 GHz) and low temperature coefficient of the resonant frequency ($\tau_f = 2$ ppm/°C) [2].

$\text{Ba}_2\text{Ti}_9\text{O}_{20}$ ceramic has a hexagonal closed packed arrangement of Ba and O atoms with Ti occupying the appropriate octahedral sites [4]. $\text{Ba}_2\text{Ti}_9\text{O}_{20}$ has triclinic space group $P\bar{1}$ with $a = 7.471(1)$ Å, $b = 14.081(2)$ Å,

$c = 14.344(2)$ Å and $\alpha = 89.94(2)^\circ$, $\beta = 79.43(2)^\circ$, $\gamma = 84.45(2)^\circ$ [5]. There are four molecules per unit cell ($Z = 4$) and there are 8 barium, 36 titanium and 80 oxygen atoms in the primitive triclinic cell. In the unit cell, titanium ions are located at octahedral sites. Four of the barium ions are 12-coordinated by oxygen, whereas the other four barium ions have a vacancy present in the adjacent barium ions which possibly improve the microwave dielectric properties of $\text{Ba}_2\text{Ti}_9\text{O}_{20}$ compared with other barium and alkali titanate structures [6].

In BaO–TiO₂ system, $\text{Ba}_2\text{Ti}_9\text{O}_{20}$ is a stable phase but it decomposes in the solid state to BaTi_4O_9 and rutile at temperatures over 1300°C [3, 4]. During formation of $\text{Ba}_2\text{Ti}_9\text{O}_{20}$ from solid state, $\text{BaTi}_5\text{O}_{11}$ is the first phase to form and then it converts to BaTi_4O_9 which then reacts with TiO₂ to form $\text{Ba}_2\text{Ti}_9\text{O}_{20}$ ceramic [7]. High temperatures are required to produce dense $\text{Ba}_2\text{Ti}_9\text{O}_{20}$ ceramics from BaCO₃ and TiO₂ by solid state mixing. The sluggish formation of $\text{Ba}_2\text{Ti}_9\text{O}_{20}$ is due to increase of distance between intermediate phases, high surface and interface energies or the high potential energy barrier due to the crystal structure [7, 8, 9, 10, 11]. The conventional high temperature sintering also leads to compositional and structural fluctuations due to reduction of Ti⁴⁺ to Ti³⁺ which degrade the dielectric properties [12]. Therefore, various methods have been applied to obtain single phase and dense $\text{Ba}_2\text{Ti}_9\text{O}_{20}$ ceramics at relatively low temperatures. One of these methods is additive addition into the $\text{Ba}_2\text{Ti}_9\text{O}_{20}$ and the other is employing chemical routes.

Various chemical methods were applied to produce $\text{Ba}_2\text{Ti}_9\text{O}_{20}$ ceramics [8, 13, 14, 15]. Sol-gel processing was applied by Lu et al. [8] and Xu et al. [16] to promote formation of $\text{Ba}_2\text{Ti}_9\text{O}_{20}$. Alkoxide precursor synthesis

was applied by Ritter et al. [13] who produced $Ba_2Ti_9O_{20}$ by sintering the precipitates obtained from the hydrolysis of mixed barium and titanium ethoxide precursors at controlled conditions. Citrate route was also used to produce $Ba_2Ti_9O_{20}$ powders [14]. In this method, the crystallization and sintering temperatures of $Ba_2Ti_9O_{20}$ was reduced due to large surface area of citrate derived precursor powders. Javadpour and Eror [17] prepared $Ba_2Ti_9O_{20}$ ceramic by a liquid mixing technique of $BaCO_3$ with tetraisopropyl titanate in a solution of ethylene glycol and citric acid and single-phase $Ba_2Ti_9O_{20}$ was obtained only after a long heat treatment at $1200^\circ C$. Xu et al. [16] used modified Pechini method where they used ethylenediamine tetraacetic acid as chelating agent and pure $Ba_2Ti_9O_{20}$ phase was produced after calcination at $1200^\circ C$ for 2-6 h. Coprecipitation techniques were also used to produce $Ba_2Ti_9O_{20}$ ceramic in which an aqueous solution of $BaCl_2$, $TiCl_4$ with H_2O_2 and $NH_3/(NH_4)_2CO_3/NH_4OH$ were used [18, 19].

In the present study, chemically homogeneous $Ba_2Ti_9O_{20}$ nanopowders were produced by a polymerised complex method using barium carbonate and titanium isopropoxide. The decomposition process of the precursor was studied by DTA-TG. Phase development was investigated by X-ray diffraction using $Ba_2Ti_9O_{20}$ precursor powders heat treated at various temperatures. The dielectric properties of sintered $Ba_2Ti_9O_{20}$ ceramics were studied.

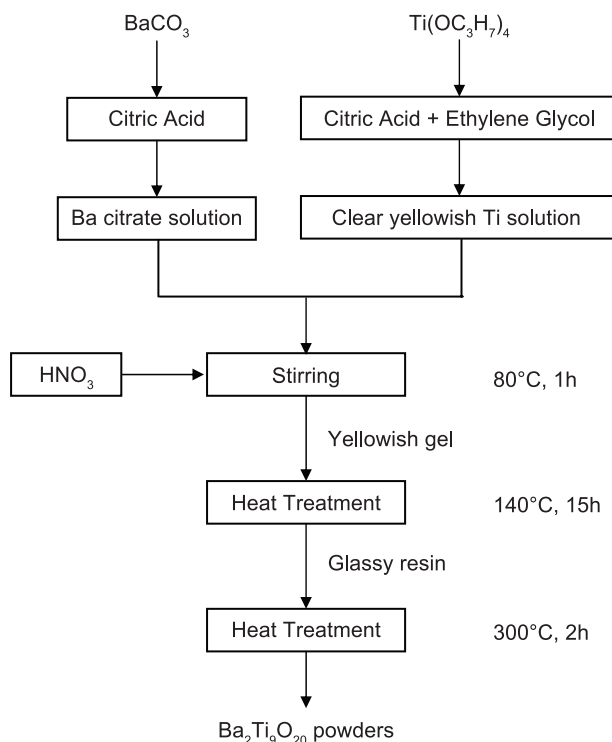


Figure 1. The flowchart for preparing $Ba_2Ti_9O_{20}$ powders using ethylene glycol and citric acid.

EXPERIMENTAL

Modified Pechini method [20] was used to produce $Ba_2Ti_9O_{20}$ ceramic from barium carbonate ($BaCO_3$, 99 %, Merck), titanium isopropoxide ($Ti(OC_3H_7)_4$, 98 %, Merck), citric acid ($C_6H_8O_7$), 99.5 %, Merck) and ethylene glycol ($HOCH_2CH_2OH$, 99 %, Merck). Figure 1 shows the flow chart for the preparation of $Ba_2Ti_9O_{20}$. While barium citrate solution was prepared by dissolving stoichiometric amounts of $BaCO_3$ in 0.6 M citric acid, stoichiometric amounts of titanium isopropoxide was dissolved in ethylene glycol-citric acid solution. The barium citrate solution was directly added to clear yellowish titanium isopropoxide-citric acid-ethylene glycol solution. A very small amount of nitric acid (HNO_3 , 65 %) was added to the mixture to catalyze the esterification between citric acid and ethylene glycol. The resultant mixture was mixed at $80^\circ C$ for 1 h during which clear yellowish gels formed. The mixture with a gel structure was heated to around $140^\circ C$ for 15 h to evaporate the solvent and promote polymerization. The gely structure changed to a dark brown glassy resin. This resin was heated to $300^\circ C$ for 2 h for charring where it converted to a black mass and then cooled to room temperature. This mass was ground in an agate mortar.

To observe the phase development during $Ba_2Ti_9O_{20}$ formation, the ground powder was heat treated between 600 - $1200^\circ C$ for 2 h with a heating and cooling rates of 10 K/min. Heat treated powders were examined using x-ray diffractometer with $CuK\alpha$ radiation (Rigaku). Differential thermal and thermogravimetric analysis (DTA-TG) (Netzsch STA 449C) were carried out to observe the decomposition process of the precursors at a heating rate of 10 K/min. The powder heat treated at $1200^\circ C$ for 2 h was examined in a scanning electron microscope (SEM, JSM-5310LV) and transmission electron microscope (TEM, Jeol 200 V). The densities of the disc-shaped ceramic pellets sintered at $1300^\circ C$ for 4 h were determined by Archimedes method. The dielectric measurements of $Ba_2Ti_9O_{20}$ ceramics were performed at frequencies from 1 kHz to 2 MHz on silver-plated discs using a high precision LCR meter. The temperature dependence of the dielectric properties between room temperature and $200^\circ C$ was measured using an automated measurement systems consisting of a PC, a HP 4284 LCR meter and a temperature chamber.

RESULTS AND DISCUSSION

Figure 2 shows the DTA-TG results for the $Ba_2Ti_9O_{20}$ precursor. The TG curve showed a continuous weight loss up to around $1100^\circ C$. The weight loss is indicative of the dehydration of the precursors (evaporation of ethylene glycol, decomposition of citric acid, decomposition of barium carbonate). The broad exothermic peak at around $356^\circ C$ is induced by carbonization or bond breaking of

the organic moieties in the precursors, together with the evolution of great amounts of gases such CO_2 . During this period, the polymer network breaks down into smaller organic moieties, and some of these compounds which do not contain any metal ions are volatilized. The exothermic peaks located at $557^\circ C$ and $678^\circ C$ were due to decomposition into the oxides which gave a weight loss in TG. XRD confirmed these results that the powder was still amorphous at $600^\circ C$ and the first oxide ($BaTi_5O_{11}$) formed at $700^\circ C$. The endothermic peaks observed at $882^\circ C$, $1029^\circ C$ and $1129^\circ C$ could be possibly due to formation of intermediate phases and formation of $Ba_2Ti_9O_{20}$.

X-ray diffraction patterns of $Ba_2Ti_9O_{20}$ polymeric precursors heat treated between 600 – $1200^\circ C$ for 2 h is given in Figure 3. The polymeric precursor was still amorphous and no distinct peak was observed at $600^\circ C$. The first peaks appeared at $700^\circ C$ belong to the $BaTi_5O_{11}$ phase. With increasing heating temperature to $800^\circ C$, the intensity of $BaTi_5O_{11}$ peaks increased and $BaTi_4O_9$

phase started to form. At $1000^\circ C$, most of the $BaTi_5O_{11}$ phase converted to $BaTi_4O_9$ and the diffraction peaks of main crystal phase, $Ba_2Ti_9O_{20}$, started to form at this temperature. In addition, another intermediate phase of $Ba_4Ti_{13}O_{30}$ also appeared at $1000^\circ C$. At $1200^\circ C$, all the phases converted to $Ba_2Ti_9O_{20}$ and nearly single phase $Ba_2Ti_9O_{20}$ was formed. In the literature, it was also reported that during formation of $Ba_2Ti_9O_{20}$, $BaTi_5O_{11}$ was the first phase to form and then it converted to $BaTi_4O_9$, which then reacted with TiO_2 to form $Ba_2Ti_9O_{20}$ ceramic [7, 21].

SEM micrographs of $Ba_2Ti_9O_{20}$ powders calcined at $1200^\circ C$ for 2 h is depicted in Figure 4. Powder particles were submicron in size with highly agglomerated morphology which occurred due to high calcinations temperature. The fine details and morphology of $Ba_2Ti_9O_{20}$ powders calcined at $1200^\circ C$ were investigated by TEM (Figure 5). Powders had spherical morphology with a particle size between 10–50 nm. The powders also had strong agglomeration.

The crystallite size was calculated from x-ray peak broadening (Figure 3) using the Scherrer's formula ($D = K\lambda/B\cos\theta$) where D is the average size of the particles, assuming particles are spherical, $K = 0.9$, λ is the wavelength of x-ray radiation (for $CuK\alpha$, $\lambda = 1.5406 \text{ \AA}$), B is the full width at half maximum of the diffracted peak. The calculated value was 30 nm which was in agreement with TEM results.

The dielectric properties of $Ba_2Ti_9O_{20}$ ceramic sintered at $1300^\circ C$ for 4 h with a relative density of 96 % were measured. Dielectric constant indicated a sharp decrease at low frequency range of 1 kHz–250 kHz and then showed a slight decrease with frequency until 2 MHz (Figure 6a). This could be due to the phenomena of frequency dispersion [22]. At higher frequencies, the

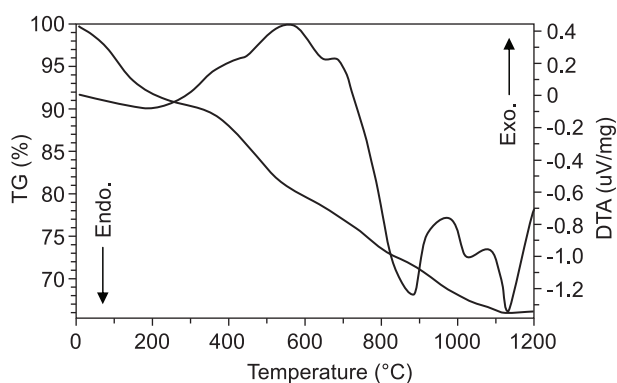


Figure 2. TG-DTA curves for the $Ba_2Ti_9O_{20}$ precursor.

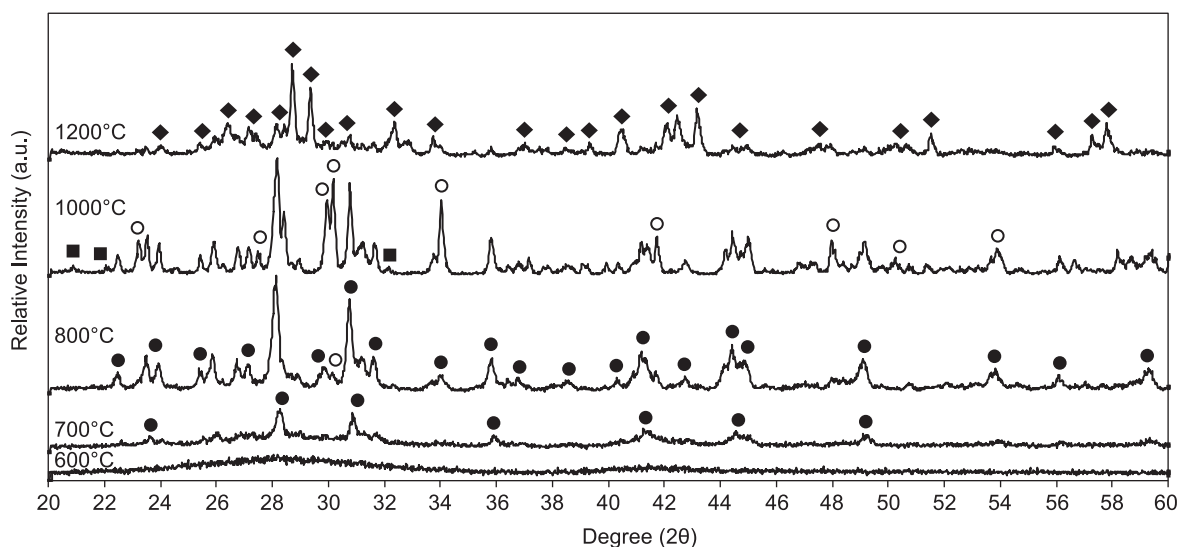


Figure 3. X-ray diffraction pattern of $Ba_2Ti_9O_{20}$ ceramic produced from modified Pechini method and heat treated at various temperatures for 2 h (● = $BaTi_5O_{11}$, ■ = $Ba_4Ti_{13}O_{30}$, ○ = $BaTi_4O_9$, ◆ = $Ba_2Ti_9O_{20}$).

frequency of hopping between the ions could not follow the applied field frequency and it lags behind the applied field frequency, hence the values of dielectric constant normally decrease at higher frequencies. The dielectric loss values were quite high and generally increased with frequency (Figure 6b). The dielectric properties were also investigated as a function of temperature. The dielectric properties increased with increasing temperature. Although room temperature dielectric constant was around 34.5 at frequencies above 250 kHz and was stable until 2 MHz, it significantly decreased when temperature rose above 25°C. In addition, the dielectric

loss increased considerably above room temperature.

CONCLUSIONS

$\text{Ba}_2\text{Ti}_9\text{O}_{20}$ nanocrystals were prepared by a polymerized complex method (or modified Pechini method). Single phase $\text{Ba}_2\text{Ti}_9\text{O}_{20}$ was obtained at 1200°C through formation of intermediate phases ($\text{BaTi}_5\text{O}_{11}$, BaTi_4O_9 and $\text{Ba}_4\text{Ti}_{13}\text{O}_{30}$). TEM results indicated that the powders heat treated at 1200°C had a particle size in the range of 10-50 nm with spherical shape. The dielectric constant of $\text{Ba}_2\text{Ti}_9\text{O}_{20}$ ceramics decreased sharply at low frequency range (1 kHz-250 kHz) and then showed a slight decrease

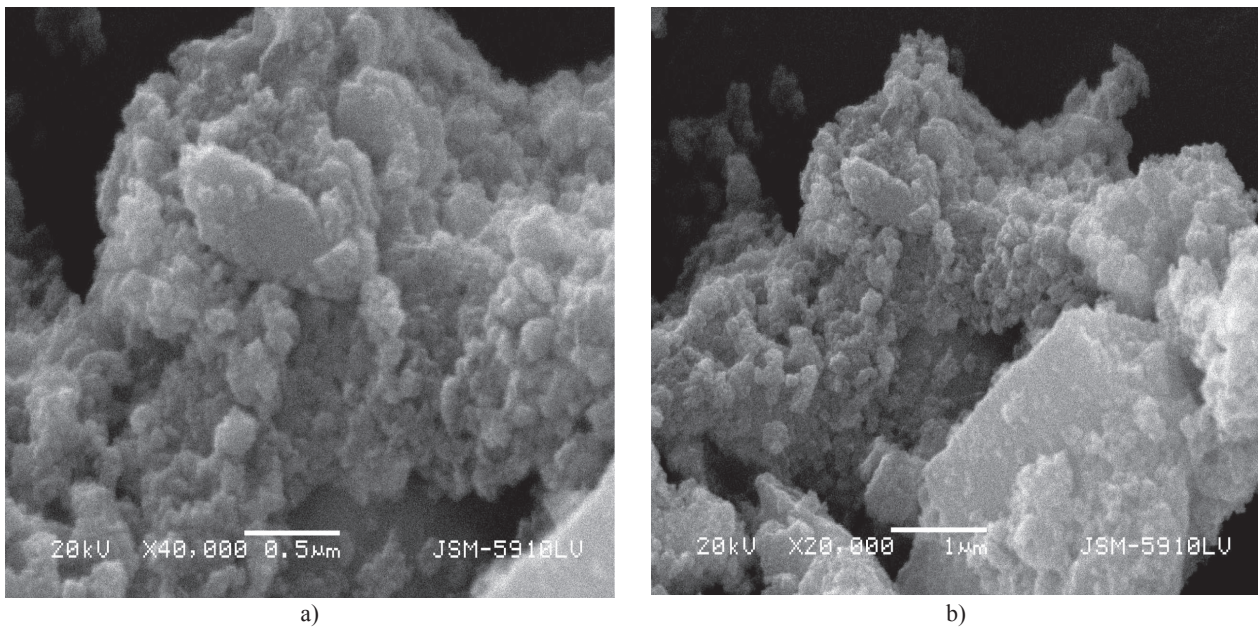


Figure 4. SEM image of $\text{Ba}_2\text{Ti}_9\text{O}_{20}$ powders calcined at 1200°C for 2 h.

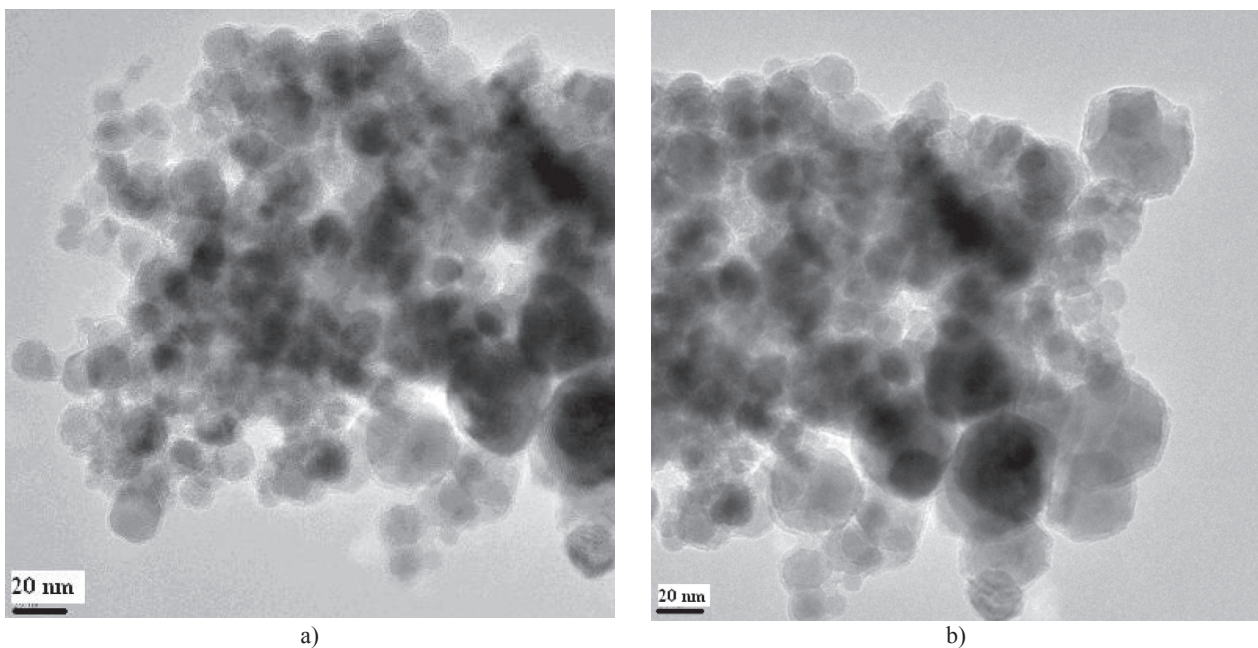


Figure 5. TEM image of $\text{Ba}_2\text{Ti}_9\text{O}_{20}$ powders calcined at 1200°C for 2 h.

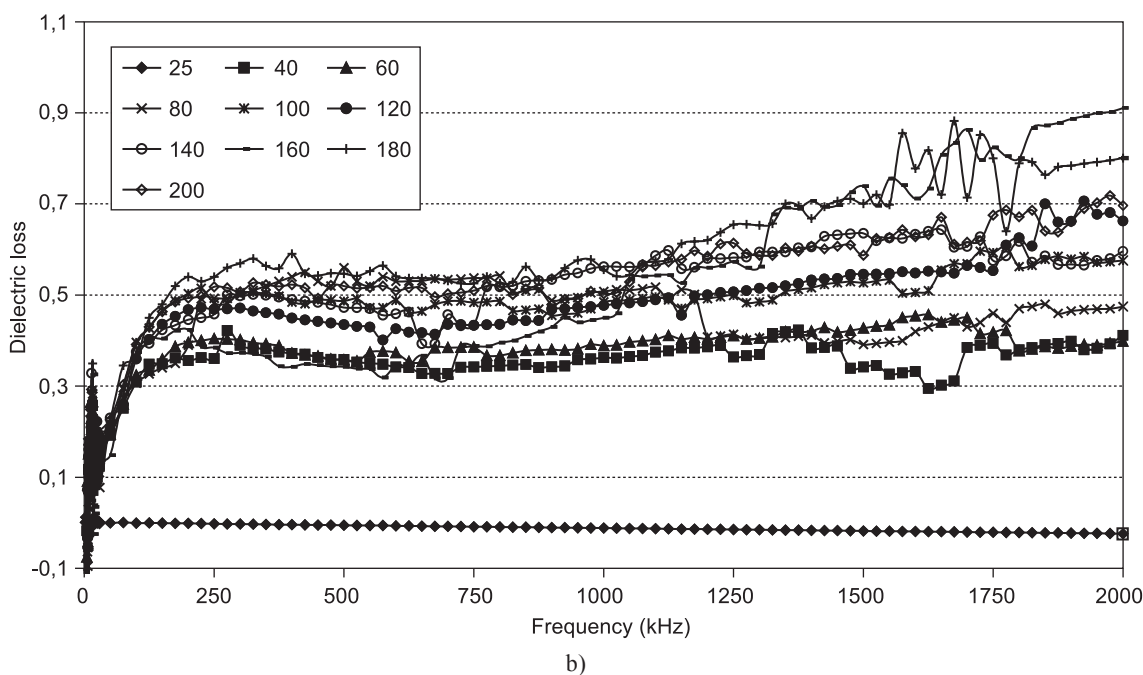
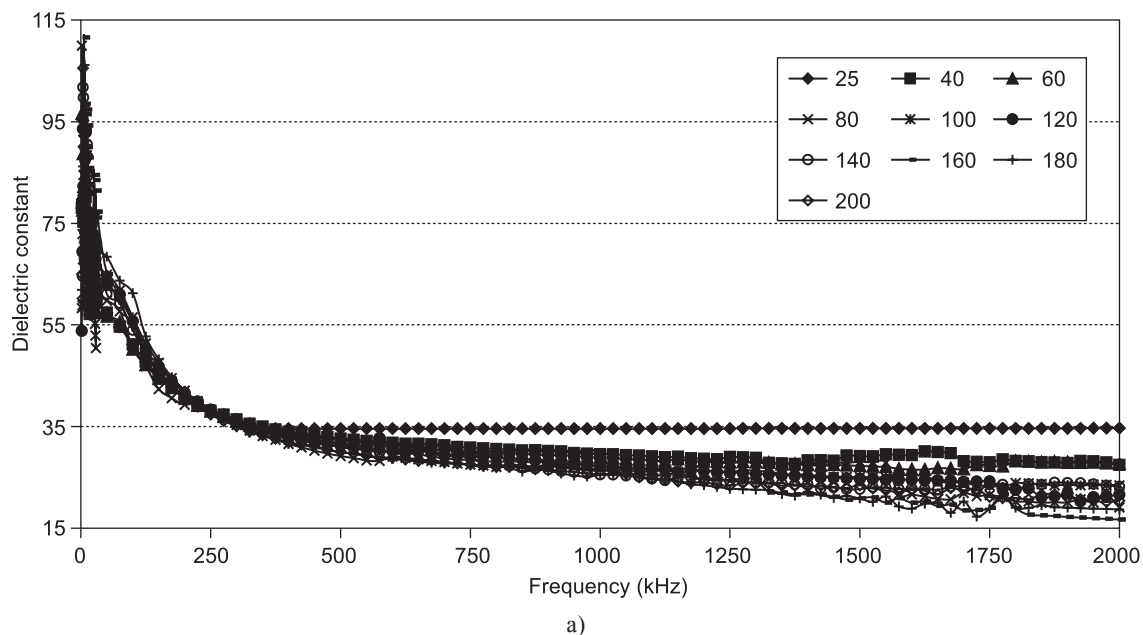


Figure 6. The change of a) dielectric constant and b) dielectric loss of $Ba_2Ti_9O_{20}$ ceramics sintered at $1300^{\circ}C$ for 4 h in a frequency range of 1 kHz-2MHz.

with frequency until 2 MHz.

Acknowledgement

I would like to give my great thanks to Marmara University Research Fund (Project No: FEN-BGS-060907-0193) for financial support of this investigation.

References

1. Jonker G. H., Kwestroo W.: J. Am. Ceram. Soc. 41, 390 (1958).
2. O'Bryan H. M., Thomson J.: J. Am. Ceram. Soc. 57, 450 (1974).
3. O'Bryan H. M., Thomson J.: J. Am. Ceram. Soc. 57, 522 (1974).
4. Negas T., Roth R. S., Parker H. S., Minor D.: J. Solid State Chem. 9, 297 (1974).
5. Tillmanns E., Hofmeister W., Baur W. H.: J. Am. Ceram. Soc. 66, 268 (1983).
6. Grzanic G., Bursill L. A., Smith D. J.: J. Solid State Chem. 47, 151 (1983).
7. Wu J. M., Wang H. W.: J. Am. Ceram. Soc. 71, 869 (1988).
8. Lu H. C., Burkhart L. E., Schrader G. L.: J. Am. Ceram. Soc. 66, 268 (1983).

- Soc. 74, 968 (1991).
9. Lin W. Y., Speyer R. F.: *J. Mater. Res.* 14, 1939 (1999).
10. Jaakola T., Uusimaki A., Leppavuori S.: *Int. J. High Technol. Ceram.* 2, 195 (1980).
11. Yu J., Zhan H., Wang J., Xia F.: *J. Am. Ceram. Soc.* 77, 1052 (1994).
12. O'Bryan H. M., Thomson H.: *J. Am. Ceram. Soc.* 66, 66 (1983).
13. Ritter J. J., Roth R. S., Blendell J. E.: *J. Am. Ceram. Soc.* 69, 155 (1986).
14. Choy J. H., Han Y. S., Sohn J. H., Itoh M. J.: *J. Am. Ceram. Soc.* 78, 1169 (1985).
15. Virkar A. N., Chatterjee C., Paul A.: *J. Mater. Sci. Lett.* 7, 179 (1988).
16. Xu Y. B., He Y. Y.: *J. Mater. Res.* 16, 1195 (2001).
17. Javadpour J., Eror N. G.: *J. Am. Ceram. Soc.* 71, 206 (1988).
18. Pfaff G.: *J. Mater. Sci. Lett.* 12, 32 (1993).
19. Chu L. W., Hsiue G. H., Lin I. N.: *J. Euro. Ceram. Soc.* 26, 2081 (2006).
20. Pechini M. P.: US Patent No: 3330697, 1967.
21. Lin W. Y., Speyer R. F., Hackenberger W. S., Shrout T. R.: *J. Am. Ceram. Soc.* 82, 1207 (1999).
22. Narang S. B., Kaur D., Bahel S.: *Mat. Lett.* 60, 3179 (2006).
-